

สมบัติโพลาริเซชันเชิงแสงของจุดควอนตัมที่เรียงกันในแนวข้าง

นางสาวนันธิดา ชิตสเว

วิทยานิพนธ์นี้เป็นส่วนหนึ่งของการศึกษาตามหลักสูตรปริญญาวิศวกรรมศาสตรดุษฎีบัณฑิต

สาขาวิชาวิศวกรรมไฟฟ้า ภาควิชาวิศวกรรมไฟฟ้า

คณะวิศวกรรมศาสตร์ จุฬาลงกรณ์มหาวิทยาลัย

ปีการศึกษา 2550

ลิขสิทธิ์ของจุฬาลงกรณ์มหาวิทยาลัย

OPTICAL POLARIZATION PROPERTY OF
LATERALLY ALIGNED QUANTUM DOTS

Miss Nan Thidar Chit Swe

A Dissertation Submitted in Partial Fulfillment of the Requirements
for the Degree of Doctor of Philosophy Program in Electrical Engineering

Department of Electrical Engineering

Faculty of Engineering

Chulalongkorn University


Academic Year 2007

Copyright of Chulalongkorn University

501280


Thesis Title OPTICAL POLARIZATION PROPERTY OF LATERALLY
 ALIGNED QUANTUM DOTS
By Miss Nan Thidar Chit Swe
Department Electrical Engineering
Thesis Advisor Chanin Wissawinthanon, Ph.D.
Thesis Co-advisors Professor Somsak Panyakeow, D.Eng.
 Professor Yasuhiko Arakawa, Ph.D.


Accepted by the Faculty of Engineering, Chulalongkorn University in Partial
Fulfillment of the Requirements for the Doctoral Degree



..... Dean of the Faculty of Engineering
(Associate Professor Boonsom Lerdhirunwong, Dr.Eng.)

THESIS COMMITTEE



..... Chairman
(Professor Vifulh Sa-yakanit, Ph.D.)


..... Thesis Advisor
(Chanin Wissawinthanon, Ph.D.)


..... Thesis Co-advisor
(Professor Somsak Panyakeow, D.Eng.)






..... Thesis Co-advisor
(Professor Yasuhiko Arakawa, Ph.D.)


..... Member
(Associate Professor Montri Sawadsarngkarn, Dr.Eng.)


..... External Member
(Noppawan Tanpipat, Ph.D.)

นันธิดา ชิตสเว : สมบัติโพลาไรเซชันเชิงแสงของจุดควอนตัมที่เรียงกันในแนวข้าง. (OPTICAL POLARIZATION PROPERTY OF LATERALLY ALIGNED QUANTUM DOTS) อ. ที่ปรึกษา: อ. ดร.ชนินทร์ วิชวินธานนท์, อ. ที่ปรึกษาร่วม: ศ. ดร.สมศักดิ์ ปัญญาแก้ว, PROF. YASUHIKO ARAKAWA, 130 หน้า.

วิทยานิพนธ์นี้มุ่งศึกษาสมบัติโพลาไรเซชันเชิงแสงของโครงสร้างจุดควอนตัมที่เรียงกันในแนวข้าง 3 แบบ ได้แก่ จุดควอนตัมคู่ จุดควอนตัมที่เรียงกันเป็นเส้นตรง และจุดควอนตัมที่เรียงกันเป็นเส้นตารางไขว้ โดยวิเคราะห์สมบัติดังกล่าวทั้งจากการคำนวณทางทฤษฎี และจากการวัดสเปกตรัมการเปล่งแสงของชิ้นงานตัวอย่าง ผลการคำนวณพบว่าหากจุดควอนตัมอยู่ใกล้กันมากขึ้น จุดควอนตัมมีขนาดเล็กลง และ/หรือจุดควอนตัมเรียงกันเป็นจำนวนมากขึ้น จะส่งผลให้ระดับชั้นโพลาไรเซชันเชิงเส้น (degree of linear polarization) ยังมีค่าเพิ่มขึ้น แต่ในกรณีที่จุดควอนตัมโคด ระดับชั้นโพลาไรเซชันจะขึ้นอยู่กับสถานะของจุดควอนตัม เช่น ถ้าจุดควอนตัมมีสถานะเป็นทรงรีในทิศทางใดทิศทางหนึ่ง แสงที่เปล่งออกมาจากจุดควอนตัมนั้นๆ ก็อาจมีค่าระดับชั้นโพลาไรเซชันที่ไม่เป็นศูนย์ได้ ผลการทดลองพบว่า ระดับชั้นโพลาไรเซชันของจุดควอนตัมคู่และจุดควอนตัมที่เรียงกันเป็นเส้นตรงมีค่าเปลี่ยนไปตามอุณหภูมิต่างกัน พฤติกรรมเช่นนี้อธิบายได้ว่าเป็นผลเนื่องจากการควบกัน (coupling) ของจุดควอนตัม แต่ค่าระดับชั้นโพลาไรเซชันที่วัดได้จากจุดควอนตัมที่เรียงกันเป็นเส้นตารางไขว้ไม่ขึ้นกับอุณหภูมิ ซึ่งเมื่อศึกษาภาพถ่ายจากกล้องจุลทรรศน์ชนิดแรงอะตอม (atomic-force microscope) พบว่าจุดควอนตัมในชิ้นงานตัวอย่างชนิดนี้เรียงกันเป็นแถวยาว แต่จุดควอนตัมไม่อยู่ใกล้กันเพียงพอที่จะก่อให้เกิดการควบกัน แสดงว่าค่าระดับชั้นโพลาไรเซชันที่เกิดขึ้นนั้นมีสาเหตุมาจากสถานะที่ไม่เป็นเอกรูป (non-uniform) ของจุดควอนตัมแต่ละจุด การศึกษาเปรียบเทียบและวิเคราะห์ผลที่รวบรวมได้เหล่านี้ทำให้เราเข้าใจฟิสิกส์ของสมบัติโพลาไรเซชันเชิงแสงของโครงสร้างระดับนาโนเมตรเหล่านี้ได้ดียิ่งขึ้น ซึ่งจะเป็นอย่างนี้จะเป็นองค์ความรู้พื้นฐานส่วนหนึ่งที่จะนำไปสู่การประดิษฐ์สิ่งประดิษฐ์ทางแสงที่มีประสิทธิภาพสูงสำหรับโลกในยุคนาโนเทคโนโลยีต่อไป

ภาควิชา	วิศวกรรมไฟฟ้า	ลายมือชื่อนิสิต	
สาขาวิชา	วิศวกรรมไฟฟ้า	ลายมือชื่ออาจารย์ที่ปรึกษา	
ปีการศึกษา	2550	ลายมือชื่ออาจารย์ที่ปรึกษาร่วม	
		ลายมือชื่ออาจารย์ที่ปรึกษาร่วม	

4771873021 : MAJOR ELECTRICAL ENGINEERING

KEY WORD: QUANTUM DOTS/ MOLECULAR-BEAM EPITAXY/ PHOTO-LUMINESCENCE/ LINEAR POLARIZATION DEGREE/ COUPLING


NAN THIDAR CHIT SWE: OPTICAL POLARIZATION PROPERTY OF LATERALLY ALIGNED QUANTUM DOTS. THESIS ADVISOR: CHANIN WISSAWINTHANON, THESIS COADVISORS: PROF. SOMSAK PANYAKEOW, PROF. YASUHIKO ARAKAWA, 130 pp.


This work emphasizes on the optical polarization property of three kinds of quantum dot (QD) structures, namely, binary quantum dots (bi-QDs), linearly aligned quantum dots (LAQDs), and QDs aligned on a cross-hatch pattern. Such property was investigated by means of photoluminescence spectroscopy as well as theoretical calculation. It was found out from calculation that linear polarization degree (PD) of the LAQDs strongly depends on spacing, size, and number of QDs in the alignment. In particular, closer spacing, smaller dot size, or more number of QDs in the alignment gives rise to a higher PD value. For isolated QDs, the extent of shape isotropy strongly affects the PD. In the experimental point of view, optical properties of the three kinds of structures were investigated by means of temperature-dependent-, excitation-power-dependent-, and polarization-resolved photoluminescence spectroscopy. Measurements on a bi-QD sample and two LAQD samples reveal that the temperature-dependent PD for these nanostructures originates from coupling among the QDs. On the other hand, QDs on a cross-hatch pattern did not show the temperature-dependent behavior; the amount of PD that was observed for this type of sample merely comes from the shape anisotropy of individual QDs. By comparing these results, the physics behind the observed behaviors of these nanostructures is better understood and this will help produce higher-efficiency devices for the era of nanotechnology.


DepartmentElectrical Engineering..

Field of study ..Electrical Engineering..

Academic year2007.....

Student's signature

Advisor's signature

Co-advisor's signature

Co-advisor's signature

Acknowledgements

First and foremost, I would like to express my deep gratitude to my parents who are my first teachers in my life. My special appreciation goes to my principal thesis advisor Dr. Chanin Wissawinthanon and my thesis co-advisor Professor Dr. Somsak Panyakeow, for their research insight, critical questions and frank advice, and for setting an example of creativity, and for dedication to this student who worked with them. They guided me with enthusiasm, encouraged me to continue doing research, transferred knowledge to me, and mentored me in all aspects.

I am very grateful to acknowledge Dr. Suwaree Suraprapich and Dr. Cho Cho Thet for their MBE-grown quantum-dot samples used in my optical characterization study, Mr. Supachok Thanoi for helping me in my experiments, and all of my teachers from SDRL: Dr. Montri Sawadsaringkarn, Dr. Choopol Antarasena, Dr. Somchai Ratanathamphan, and Dr. Songphol Kanjanachuchai, for their teaching, valuable advice and discussions. My special thanks go to the chairman of my thesis defense Professor Dr. Virulh Sa-yakanit (Professor Emeritus from Department of Physics) and the external committee member Dr. Noppawan Tanpipat (Deputy Director of National Nanotechnology Center of Thailand).

Specifically, I am also greatly indebted into my thesis co-advisor Professor Dr. Yasuhiko Arakawa, University of Tokyo, Japan, for accepting me as a research student at the Arakawa-Iwamoto Laboratory. I would like to also acknowledge Dr. Saitoshi Iwamoto for advising me how to make good optical setup, Dr. Masahiro Nomura and Dr. Saitoshi Kako for helping me to know more about optics and giving me very useful advice. Many thanks here also go to my special friends: Aniwat Tandaechanurat, Dr. Luigi Martriadonna, and Christain Kindel, for their help, kind encouragements, support and friendship, and vivid memory during my stay at Arakawa-Iwamoto Laboratory.

Finally, I would like to acknowledge the Japan International Cooperation Agency (JICA) for ASEAN University Network / South-East Asia Engineering Education Development Network (AUN/SEED-Net), Asian Office for Aerospace Research and Development (AOARD) of the Air Forces of the United States of America, Thailand Research Fund (TRF), National Nanotechnology Center (NANOTEC) of Thailand, Chulalongkorn University, and University of Tokyo, for their financial support and cooperation.

CONTENTS

	Page
Abstract (Thai)	iv
Abstract (English)	v
Acknowledgements.....	vi
Contents.....	vii
List of Tables	xi
List of Figures	xii
Chapter I Introduction	1
1.1 Background.....	1
1.2 Quantum Dots: the Artificial Atoms.....	2
1.3 Ordered Quantum Dots.....	3
1.4 Ordered Quantum Dots for Quantum-Dot-Based Photonic Devices.....	4
1.5 Objectives.....	5
1.6 Scope of Work.....	5
1.7 Research Methodology.....	6
1.8 Significance of the Research.....	6
1.9 Work Presented in This Thesis.....	7
Chapter II Low-Dimensional Semiconductor Nanostructures: Quantum Confinement and Its Effect on Optical Properties.....	8
2.1 Basic Concepts of Low-Dimensional Nanostructures	8
2.1.1 Bulk Material.....	10
2.1.2 Quantum Wells.....	10
2.1.3 Quantum Wires.....	11
2.1.4 Quantum Dots.....	12
2.1.5 Quantum Rings.....	12
2.2 Effect of Quantum Confinement on Optics of Semiconductor Nanostructures.....	13
2.2.1 Size Effect on Optical Properties.....	15
2.2.2 Increase of Oscillator Strength.....	16

	Page
2.2.3 New Intraband Transition.....	16
2.2.4 Increased Exciton Binding Energy.....	17
2.2.5 Dielectric Confinement Effect.....	17
2.2.6 Increase of Transition Probability in Indirect Bandgap Semiconductors.....	18
2.2.7 Nonlinear Optical Properties Caused by the Quantum Confinement Effect.....	18
2.3 Quantum Dots and Physics Behind them.....	18
2.3.1 Energy Levels.....	19
2.3.1 Spontaneous Emission.....	21
2.3.2 Polarization Properties.....	25
 Chapter III Numerical Calculation	 26
3.1 Mathematical Approach.....	26
3.2 Mathematical Model.....	26
3.3 Theory.....	27
3.4 Numerical Method.....	28
3.4.1 One-dimensional Schrödinger Equation	28
3.4.2 Two-dimensional Rectangular Dots.....	30
3.5 Results and Discussion.....	32
3.5.1 Energy Splitting Behavior.....	32
3.5.2 Effect of Coupling on the Linear Optical Polarization Property.....	35
3.5.2.1 Single Quantum Dots.....	36
3.5.2.2 Binary Quantum Dots.....	39
3.5.2.3 Increase of Polarization Degree with Number of QDs.....	44
3.6 Conclusion.....	45
 Chapter IV Photoluminescence Spectroscopy.....	 46
4.1 Photoluminescence.....	46
4.2 Optical Excitation.....	50

	Page
4.3 Macro-Photoluminescence.....	52
4.4 Micro-Photoluminescence.....	53
4.4.1 Cryogenics.....	53
4.3.2 Optical Setup.....	56
4.3.3 Temperature Effect.....	61
4.5 Polarized-PL Measurements.....	63
4.5.1 Malus's Law.....	63
4.5.2 Polarized-PL Experimental Setup.....	64
 Chapter V Optical Characterization of Aligned Quantum Dots.....	 67
5.1 Self-Assembly Crystal Growth.....	67
5.2 Thin-Capping and Re-Growth Technique.....	68
5.2.1 (a) As-Grown QDs (Reference Sample).....	68
5.2.1 (a) High-Density QDs (Reference Sample).....	69
5.2.2 Binary Quantum Dot.....	71
5.2.2.1 Excitation-Power-Dependent PL Measurement	72
5.2.2.2 Temperature-Dependent PL Measurements.....	74
5.2.2.3 Polarization-Resolved PL Measurements.....	75
5.2.2.4 Single Dot Spectroscopy.....	78
5.2.3 Linearly Aligned Quantum Dots.....	81
5.2.3.1 Sample 0434 (Sample A).....	81
5.2.3.2 Sample 070081 (Sample C).....	84
5.2.3.3 Sample 070080 (Sample B).....	86
5.2.3.4 Comparison of Three Laterally Aligned QD Structures and the Effects of Growth Parameters on their Optical Properties.....	 88
5.2.3.5 Polarization- Resolved PL Measurements of Aligned QDs.....	 91
5.3 Optical Characterization of QDs on a Cross-Hatch Virtual Substrate.....	 94
5.3.1 Sample 0607 (Sample X1).....	95
5.3.2 Sample 0620 (Sample X2).....	97

	Page
5.3.3 Polarization-Resolved PL Measurements.....	99
5.3.3.1 Sample X1.....	99
5.3.3.2 Sample X2.....	100
5.3.4 Temperature-Dependent PL Measurement of Sample X1.....	101
5.4 Overall Discussion	106
 Chapter VI Conclusion.....	 108
 References.....	 111
Appendices.....	122
Appendix A: Matlab® Program.....	123
Appendix B: List of Publications.....	129
Vitae.....	130

LIST OF TABLES

	Page
Table 2.1 Quantum confined behavior of semiconductor nanostructures.....	9
Table 3.1 Comparison between the analytical and the numerical methods.....	32
Table 3.2 The polarization degree vs. dot aspect ratio of single QDs.....	38
Table 3.3 The polarization degree of binary quantum dots with various interdot spacings. The middle number refers to the interdot spacing (that is, the barrier width between the dots).....	41
Table 3.4 The polarization degree of binary quantum dots with various dot sizes. The dot size was varied from 8 nm to 44 nm while the interdot spacing was fixed at 2 nm.....	42
Table 3.5 The polarization degree vs the number of QDs aligned in the x direction. The dot size was maintained at 12 nm \times 12 nm (isotropic shape) and the interdot spacing between adjacent QDs was fixed at 2 nm. The number of dots increased in the x direction	44
Table 5.1 Summary of the optical characterization of as-grown QDs and high- density QDs.....	70
Table 5.2 Summary of growth parameters for three laterally aligned QD samples.....	88
Table 5.3 Summary of PL of three laterally aligned QD Samples measured at room and low temperatures	88
Table 5.4 Summary of linear polarization degree versus temperature for Sample A, Sample B, and Sample C.....	94
Table 5.5 Dimensions of five representative QDs on a cross hatch pattern (Sample X) from SEM measurement.....	95
Table 5.6 Distance between one QD and its neighbor on the cross-hatch pattern (Sample X) from SEM measurements at five locations on the sample.....	95
Table 5.7 Polarization degree of Sample X1 measured at five different locations on the sample.....	100

LIST OF FIGURES

		Page
Figure 2.1	Progressive generation of rectangular nanostructures.....	9
Figure 2.2	Progressive generation of curvilinear nanostructures.....	9
Figure 2.3	Nature of electron density of states in bulk, quantum well, quantum wire, and quantum dot.....	13
Figure 2.4	Intraband and Interband scattering of an electron from initial state to final state.....	14
Figure 2.5	(a) Schematic diagram of an absorption process where a photon is absorbed (destroyed) and the energy and the momentum of the electron is altered (upper figure) (b) The emission of a photon where a photon is created (lower figure).....	15
Figure 2.6	Energy band diagram of quantum dot: A radiative transition from the lowest energy level in the conduction band to the highest energy level in the valence band is indicated.....	20
Figure 3.1	(a) An AFM image of InAs/GaAs linearly aligned quantum dots, and (b) the corresponding schematic diagram.....	26
Figure 3.2	Schematic diagram of the model for linearly aligned quantum dots	27
Figure 3.3	Three-point finite-difference approximation used to discretize the wavefunction and the potential energy.....	28
Figure 3.4	The discretized mesh points for the two-dimensional Schrödinger equation	30
Figure 3.5	Dot-separation-dependent energy splitting behavior for (a) four, (b) five, and (c) six QDs; and (d) difference in energy of the top-most and the bottom-most ground-state levels versus the number of QDs.....	33
Figure 3.6	One-dimensional (left) and two-dimensional (right) coupling behavior of six coupled QDs with dot separation (a) 10 nm, and (b) 6 nm	34
Figure 3.7	The maximum coupling caused by coalescence of six coupled QDs	34

	Page
Figure 3.8	The ground-state electron wavefunction of an isotropic single quantum dot whose size is 12 nm× 12 nm. 36
Figure 3.9	The ground-state electron wavefunction of an elongated QD (the size in the x direction was elongated to 36 nm while that in the y direction was maintained at 12 nm) 37
Figure 3.10	The polarization degree for a single QD whose size in the x direction was elongated from 12 nm to 108 nm while that in the y direction was maintained at 12 nm. 37
Figure 3.11	Schematic diagram of binary quantum dots, each of size $a \times a$ nm ² and interdot spacing d nm..... 39
Figure 3.12	The ground-state electron wavefunction of binary quantum dots, each of size 12 nm×12 nm with an interdot spacing of 2 nm..... 40
Figure 3.13	The ground-state electron wavefunction of binary quantum dots, each of size 12 nm×12 nm with an interdot spacing of 12 nm..... 41
Figure 3.14	The polarization degree of binary quantum dots vs. their interdot spacing (the dot size was fixed at 12 nm ×12 nm and the interdot spacing was varied from 0 nm to 22 nm). 42
Figure 3.15	The polarization degree of binary quantum dots with various dot sizes. The dot size was varied from 8 nm to 44 nm while interdot spacing was fixed at 2 nm. 43
Figure 3.16	The polarization degree vs. the number of QDs aligned in the x direction. The dot size was maintained at 12 nm ×12 nm (isotropic shape) and the interdot spacing between adjacent QDs was fixed at 2 nm. The number of dots increased in the x direction..... 44
Figure 4.1	A typical energy diagram for electron system. As the incident light (EM radiation) strikes on the sample, it causes electrons to jump up into excited states 47

	Page
Figure 4.2	A typical energy absorption diagram in direct- and indirect-bandgap semiconductors: As the incident light (EM radiation) strikes on the sample, it causes electrons to jump up from the valance band into the conduction band. 49
Figure 4.3	A typical energy emission diagram in direct- and indirect-bandgap semiconductors: As electrons come back to the initial state in the valence band, the electron and the holes recombine and emit photoluminescence 49
Figure 4.4	Bandgap energy changes due to impurity and other effects..... 50
Figure 4.5	Non-resonant optical excitation..... 52
Figure 4.6	Macro-photoluminescence setup..... 52
Figure 4.7	Standard lock-in technique 53
Figure 4.8	Cross-section of the cryostat..... 54
Figure 4.9	(a) Schematic diagram of the cooling system for the sample..... 54 (b) Photo of cooling system for the sample used in this work..... 55
Figure 4.10	Schematic diagram of the micro-PL setup..... 59
Figure 4.11	(a) Photo of the micro-PL setup and its components..... 60 (b) Close-up photo of the micro-PL setup and its components 60
Figure 4.12	Schematic diagram of a setup for the temperature-dependent measurement 61
Figure 4.13	Photo of the temperature-dependent PL setup 62
Figure 4.14	Explanation for linear polarization 63
Figure 4.15	Experimental setup for polarization measurements..... 64
Figure 4.16	Photo of polarization measurement setup..... 65
Figure 5.1	AFM image of as-grown InAs QDs grown on semi-insulating [001] GaAs substrate (Suraprapapich <i>et al.</i> , 2005)..... 68
Figure 5.2	Polarization-resolved PL spectra of as-grown InAs QDs measured at 77 K..... 69
Figure 5.3	AFM image of high-density InAs QDs on semi-insulating [001] GaAs substrate grown by using the thin-capping-and-regrowth technique for 10 cycles (Suraprapapich <i>et al.</i> , 2005)..... 69

	Page
Figure 5.4	PL spectra of high-density InAs QDs measured at a low temperature (4 K) with the excitation power of 500 μ W..... 70
Figure 5.5	(a) AFM image of binary QDs, and (b) close-up image of binary QDs (Suraprapapich <i>et al.</i> , 2006)..... 71
Figure 5.6	Excitation-power-dependent PL spectra of bi-QDs at room temperature..... 72
Figure 5.7	Excitation-power-dependent PL spectra at 10 K, the spectrum can be convoluted into two Gaussian peaks..... 73
Figure 5.8	Temperature-dependent PL spectra of bi-QDs measured at 10 K and 90 K. The peak shift by 10 meV is clearly observed 74
Figure 5.9	Temperature-dependent integrated PL intensity of bi-QDs. The temperature ranges from 4 K to 180 K, and the laser excitation power was held at 10 μ W..... 75
Figure 5.10	Temperature-dependent polarized PL intensity of binary QDs at (a) 10 K and (b) 80 K. When the temperature was increased, the shape the spectrum changed and the polarization degree increased 76
Figure 5.11	Temperature-dependent polarization degree of binary QDs; the temperature ranges from 4 K to 180 K, and the excitation power was held at 10 μ W..... 77
Figure 5.12	Excitation-power-dependent single-dot spectroscopy of the bi-QD system; the excitation power ranges from 25 nW to 200 nW, and the temperature was held at 3.8 K. At 25 nW, three distinct peaks were observed, and when the excitation power was increased, many peaks appeared..... 78
Figure 5.13	Excitation-power-dependent single-dot spectroscopy of exciton state and bi-exciton state from single-dot spectroscopy measured at 4 K. The exposure time to measure the optical signal from the sample was 90 s..... 79
Figure 5.14	Polarization spectroscopy of single QDs in bi-QDMs. Fine structure splitting and the polarization characteristic were observed at 1.1352 eV..... 80

	Page
Figure 5.15 AFM images of (a) a camel-like structure created as a result of thin-capping and regrowing over as-grown QDs, (b) nano-template for aligned quantum dots with an average length of 0.5 μm (Suraprapapich <i>et al.</i> , 2005).....	81
Figure 5.16 AFM images of Sample A: (a) 500 \times 500 nm^2 , (b) 1 \times 1 μm^2 (Suraprapapich <i>et al.</i> , 2005).....	82
Figure 5.17 Room-temperature PL spectra of Sample A: Two peaks appeared and the third peak at 1.3 eV came from the wetting layer.....	82
Figure 5.18 Low-temperature PL spectra of Sample A (4 K).....	83
Figure 5.19 AFM images of Sample C: (a) 4 \times 4 μm^2 , (b) 1 \times 1 μm^2 . The average alignment length is 1 μm (Suraprapapich <i>et al.</i> , 2007).....	84
Figure 5.20 Room-temperature PL spectra of Sample C.....	85
Figure 5.21 Low-temperature micro-PL spectra of Sample C	85
Figure 5.22 AFM images of Sample B: (a) 2 \times 2 μm^2 (b) 1 \times 1 μm^2 for aligned quantum dots. The average length is 1 μm (Suraprapapich <i>et al.</i> , 2007).....	86
Figure 5.23 Room-temperature micro-PL spectra of Sample B	87
Figure 5.24 Low-temperature micro-PL spectra of Sample B (4K).....	87
Figure 5.25 Comparison between room-temperature micro-PL spectra of Sample A, Sample B, and Sample C. The excitation power was held at 300 μW	89
Figure 5.26 Comparison between room-temperature and low-temperature polarized micro-PL spectra for Sample A, Sample B, and Sample C	92
Figure 5.27 Comparison between polarized micro-PL spectra measured at 70K of (a) Sample B and (b) Sample C. The excitation power is held at 3.5 μW	93
Figure 5.28 AFM image of a cross-hatch virtual substrate before QDs were grown on it. (C. C. Thet <i>et al.</i> , 2007)	94
Figure 5.29 AFM image of QDs on a cross-hatch pattern. 50 nm of $\text{In}_{0.15}\text{Ga}_{0.85}\text{As}$ layer was used for the cross-hatch pattern. Because of the well-patterned substrate QDs were well aligned (C. C. Thet <i>et al.</i> , 2007).....	95

	Page
Figure 5.30	Excitation-power-dependent PL spectra of QDs on the cross-hatch (Sample X1) at 4.4 K..... 96
Figure 5.31	AFM image of QDs on a cross-hatch pattern. 100 nm of $\text{In}_{0.15}\text{Ga}_{0.85}\text{As}$ layer was used for the cross-hatch pattern. Because of the ill-patterned layer, the QDs were not well aligned (C. C. Thet <i>et al.</i> ,2007)..... 97
Figure 5.32	Excitation-power-dependent PL spectra of QDs on a cross hatch measured at 4.4 K (Sample X2) 98
Figure 5.33	Power-dependent micro-PL spectra of Sample X2. The peaks were at 1.32 eV and the emission intensity was stronger than that emitted from the QDs and the linewidths of the spectra were small..... 98
Figure 5.34	(a) Polarized-PL measurement result, which follows the Malus's law (b) Polarized-PL spectra of Sample X1 measured at low temperature (4.4 K)..... 99
Figure 5.35	(a) Polarized-PL measurement result, which follows the Malus's law, and (b) Polarized-PL spectra of Sample X2 measured at low temperature (4.4 K)..... 100
Figure 5.36	(a) Temperature-dependent PL spectra of Sample X1, and (b) Peak shift caused by the effect of temperature is clearly be seen in the figure. 102
Figure 5.37	Temperature-dependent PL measurement result showing the integrated PL intensity and peak shift for Sample X1..... 103
Figure 5.38	(a) Polarized PL spectra of QDs on the cross-hatch sample measured at 6 K, and (b) temperature-dependent polarization degree for Sample X1 (4 K to 130 K)..... 104